



Phosphoproteomics of *Aspergillus fumigatus* Exposed to the Antifungal Drug Caspofungin

Eliciane Cevolani Mattos,^a Giuseppe Palmisano,^b  Gustavo H. Goldman^a

^aFaculdade de Ciências Farmacêuticas de Ribeirão Preto, Universidade de São Paulo, Ribeirão Preto, Brazil

^bDepartamento de Parasitologia, Instituto de Ciências Biomédicas, Universidade de São Paulo, São Paulo, Brazil

ABSTRACT *Aspergillus fumigatus* is an opportunistic and allergenic pathogenic fungus, responsible for fungal infections in humans. *A. fumigatus* infections are usually treated with polyenes, azoles, or echinocandins. Echinocandins, such as caspofungin, can inhibit the biosynthesis of the β -1,3-glucan polysaccharide, affecting the integrity of the cell wall and leading to fungal death. In some *A. fumigatus* strains, caspofungin treatment at high concentrations induces an increase of fungal growth, a phenomenon called the caspofungin paradoxical effect (CPE). Here, we analyze the proteome and phosphoproteome of the *A. fumigatus* wild-type strain and of mitogen-activated protein kinase (MAPK) *mpkA* and *sakA* null mutant strains during CPE (2 μ g/ml caspofungin for 1 h). The wild-type proteome showed 75 proteins and 814 phosphopeptides (corresponding to 520 proteins) altered in abundance in response to caspofungin treatment. The $\Delta mpkA$ ($\Delta mpkA$ caspofungin/wild-type caspofungin) and $\Delta sakA$ ($\Delta sakA$ caspofungin/wild-type caspofungin) strains displayed 626 proteins and 1,236 phosphopeptides (corresponding to 703 proteins) and 101 proteins and 1,217 phosphopeptides (corresponding to 645 proteins), respectively, altered in abundance. Functional characterization of the phosphopeptides from the wild-type strain exposed to caspofungin showed enrichment for transcription factors, protein kinases, and cytoskeleton proteins. Proteomic analysis of the $\Delta mpkA$ and $\Delta sakA$ mutants indicated that control of proteins involved in metabolism, such as in production of secondary metabolites, was highly represented in both mutants. Results of functional categorization of phosphopeptides from both mutants were very similar and showed a high number of proteins with decreased phosphorylation of proteins involved in transcriptional control, DNA/RNA binding, cell cycle control, and DNA processing. This report reveals novel transcription factors involved in caspofungin tolerance.


IMPORTANCE *Aspergillus fumigatus* is an opportunistic human-pathogenic fungus causing allergic reactions or systemic infections, such as invasive pulmonary aspergillosis in immunocompromised patients. Caspofungin is an echinocandin that impacts the construction of the fungal cell wall by inhibiting the biosynthesis of the β -1,3-glucan polysaccharide. Caspofungin is a fungistatic drug and is recommended as a second-line therapy for treatment of aspergillosis. Treatment at high concentrations induces an increase of fungal growth, a phenomenon called the caspofungin paradoxical effect (CPE). Collaboration between the mitogen-activated protein kinases (MAPK) of the cell wall integrity (MapkA) and high-osmolarity glycerol (SakA) pathways is essential for CPE. Here, we investigate the global proteome and phosphoproteome of *A. fumigatus* wild-type, $\Delta mpkA$, and $\Delta sakA$ strains upon CPE. This study showed intense cross talk between the two MAPKs for the CPE and identified novel protein kinases and transcription factors possibly important for CPE. Increased understanding of how the modulation of protein phosphorylation may affect the fungal growth in the presence of caspofungin represents an important step in the development of new strategies and methods to combat the fungus inside the host.

Citation Mattos EC, Palmisano G, Goldman GH. 2020. Phosphoproteomics of *Aspergillus fumigatus* exposed to the antifungal drug caspofungin. mSphere 5:e00365-20. <https://doi.org/10.1128/mSphere.00365-20>.

Editor Aaron P. Mitchell, University of Georgia

Copyright © 2020 Mattos et al. This is an open-access article distributed under the terms of the [Creative Commons Attribution 4.0 International license](https://creativecommons.org/licenses/by/4.0/).

Address correspondence to Gustavo H. Goldman, ggoldman@usp.br.

 Caspofungin treatment at high concentrations induces an increase of fungal growth, a phenomenon called Caspofungin Paradoxical Effect. We investigate the global proteome and phosphoproteome of the *A. fumigatus* wild-type, $\Delta mpkA$, and $\Delta sakA$ strains upon CPE. @FungalSao

Received 20 April 2020

Accepted 12 May 2020

Published 27 May 2020

KEYWORDS *Aspergillus fumigatus*, caspofungin, phosphoproteomics, MAP kinases, transcription factors

Aspergillus fumigatus is an opportunistic and allergenic pathogenic fungus that is responsible for a high incidence of fungal infections in humans and several pathologies in immunocompromised individuals. Fungal infections, such as invasive aspergillosis (IA), are usually treated with polyenes, azoles, or echinocandins (1). Polyenes are fungicidal and act by disruption of the fungal cell membrane by physically binding to the membrane ergosterol, resulting in pore formation and cell death (1). Azoles affect the biosynthesis of ergosterol, causing damage to the fungal membrane and resulting in cell death by membrane lysis or inhibition of fungal growth (1). Echinocandins can inhibit the biosynthesis of the β -1,3-glucan polysaccharide, the major component of the fungal cell wall, affecting the integrity of the cell wall and leading to fungal death (1, 2). Triazoles (voriconazole, for example) have fungistatic activities and are applied as a primary treatment in invasive aspergillosis therapy, whereas echinocandins (such as caspofungin [caspo], anidulafungin, and micafungin) act as fungistatic agents and are used as a second-line drug treatment in patients with infections that are recalcitrant to the primary treatments (1–3). The emergence of *A. fumigatus* clinical isolates resistant to azoles and echinocandins has been considered a potential public health issue (4).

In some *A. fumigatus* strains, tolerance to caspofungin at high concentrations induces an increase in fungal growth, a phenomenon called the caspofungin paradoxical effect (CPE) (5, 6). Compensatory reactions such as the transcriptional stimulation of genes encoding chitin synthases and the subsequent increase of chitin content in the cell wall are due to the activation of stress-activated signaling pathways (4, 6). High caspofungin concentrations elicit a spike in cytosolic calcium, which activates calcineurin and CrzA to promote the CPE (7, 8). Upon promotion of the CPE, calcineurin dephosphorylates the transcription factor (TF) CrzA, which is translocated to the nucleus and activates the expression of chitin synthases (9). A novel basic leucine zipper ZipD transcription factor was identified to function in the calcium-calcineurin pathway and was involved in the CPE (9). Recently, we identified four transcription factors whose null mutants are susceptible to calcium and are also involved in CPE (10).

CPE is also dependent on all four *A. fumigatus* mitogen-activated protein kinases (MAPKs). The cell wall integrity (CWI) pathway involving the MAPK MpkA (2) activates the RlmA transcription factor, which regulates the expression of chitin synthase genes in response to different concentrations of caspofungin (9, 11, 12). *A. fumigatus* MAPKs, including high-osmolarity glycerol (HOG) MAPK SakA and MpkC, are also involved in CPE, activating TFs AtfA to AtfD, which are important for CPE maintenance (13, 14). The null mutant for the MAPK MpkB, homologous to yeast Fus3 (15), is more susceptible to caspofungin and had also lost the CPE (15). A cross talk interaction between SakA and MpkA has already been observed for the adaptation to caspofungin (13, 16, 17).

It has been demonstrated that *A. fumigatus* paradoxically growing hyphae emerging from microcolonies are initially devoid of β -1,3-glucan (18) but, intriguingly, that these hyphae expose β -1,3-glucan in later growth stages (18). Fks1 glucan synthase, the main target of caspofungin, relocates to the hyphal tips during these later growth stages, suggesting that β -1,3-glucan synthase activity is restored (18, 19). Interestingly, a novel mechanism has been proposed to explain this increased glucan accumulation and Fks1 relocation to the hyphal tips (20). Analysis of the lipid microenvironment of an Fks1 from an *A. fumigatus* caspofungin-resistant mutant showed an increase in the abundance of dihydrosphingosine (DhSph) and phytosphingosine (PhSph), suggesting that caspofungin induced an alteration in the composition of plasma membrane lipids surrounding Fks1 glucan synthase, rendering it resistant to echinocandins (20).

Genetic or chemical inhibition of heat shock protein 90 (Hsp90) abolished the CPE (21). Besides Hsp90, another molecular chaperone, Hsp70, is also important for the regulation of CPE together with their cochaperone Hop/StiA (22). Transcriptional

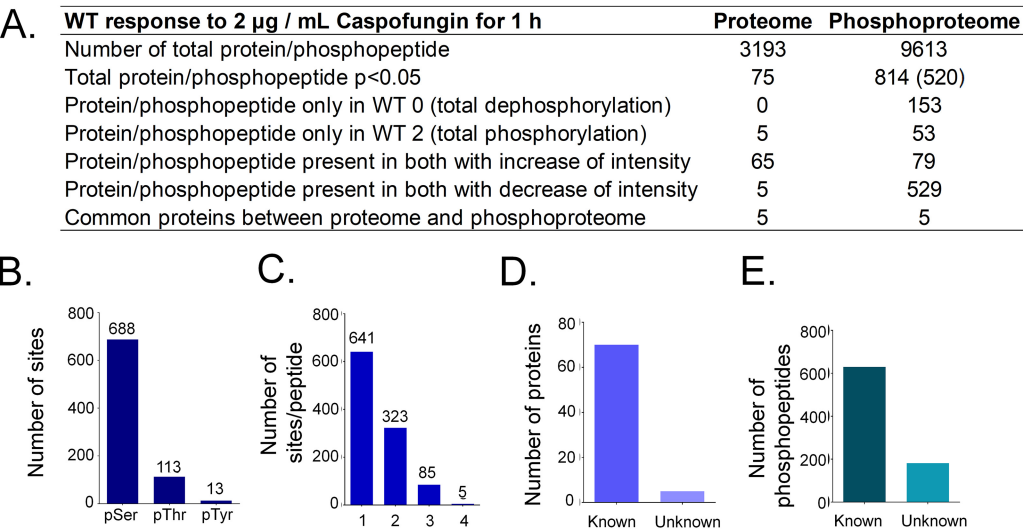


FIG 1 Proteome and phosphoproteome of *A. fumigatus* wild-type strain exposed to caspofungin. (A) Summary table of all proteins and phosphopeptides modulated in wild-type strain upon exposure to caspofungin. (B) Number of phosphorylated residues of serine, threonine, or tyrosine identified. (C) Number of sites of phosphorylation per peptide. (D) Number of proteins. (E) Number of known and unknown proteins.

profiling has shown that the main effect of reducing the Hsp90 effect is the reduction of expression of the genes of the mitochondrial respiratory chain, in particular, that of the genes encoding NADH-ubiquinone oxidoreductases (complex I) (23, 24).

The members of our laboratory are interested in understanding which genetic determinants are involved in *A. fumigatus* CPE. Recently, we evaluated the global *A. fumigatus* phosphoproteome-exposed cell wall damage mediated by Congo red (CR), identifying 485 proteins putatively involved in the cell wall stress response (25). Among these proteins, we have isolated five novel transcription factors (TFs) that were phosphorylated upon exposure to CR. The TF null mutants for three of these genes were more susceptible to CR, calcofluor white (CFW), and caspofungin with reduced CPE (25). Here, we extended these studies by analyzing the proteome and phosphoproteome of the *A. fumigatus* wild-type (WT) and $\Delta mpkA$ and $\Delta sakA$ mutant strains during the stress with caspofungin.

RESULTS

Proteome and phosphoproteome analysis of *A. fumigatus* upon caspofungin stress. The study of proteins and their posttranslational modifications in an organism under some stress conditions provided an important insight into the biological processes and signaling pathways modulated during the environmental response. Previously, we had observed that fungal mycelia grown in liquid cultures are more susceptible to high concentrations of caspofungin, and in agreement, the CPE of *A. fumigatus* strain CEA17 was already observed at 2 μ g/ml caspofungin in liquid minimal medium (MM) for 1 h, whereas the onset of the CPE was observed at 8 μ g/ml on solid medium (9). To understand how *A. fumigatus* reacts to CPE concentrations and about the involvement of MAPKs in that response, we perform proteomic and phosphoproteomic analysis of the wild-type, $\Delta sakA$, and $\Delta mpkA$ strains left untreated (control) or treated with 2 μ g/ml caspofungin for 1 h.

To understand the signaling pathways and identify new targets that may be involved in the fungal response to caspofungin, we started our study by the analysis of the wild-type response to the drug. The analysis of total proteins identified 3,193 unique proteins. The wild-type proteome showed that 75 proteins were altered in abundance in response to 2 μ g/ml caspofungin treatment, with most of them showing increased total levels (70 proteins with increased versus 5 proteins with decreased total levels) (Fig. 1A; see also Table S1A at <https://doi.org/10.6084/m9.figshare.12315212>).

Phosphoproteome Wild-type caspofungin 2 µg/ml / wild-type control

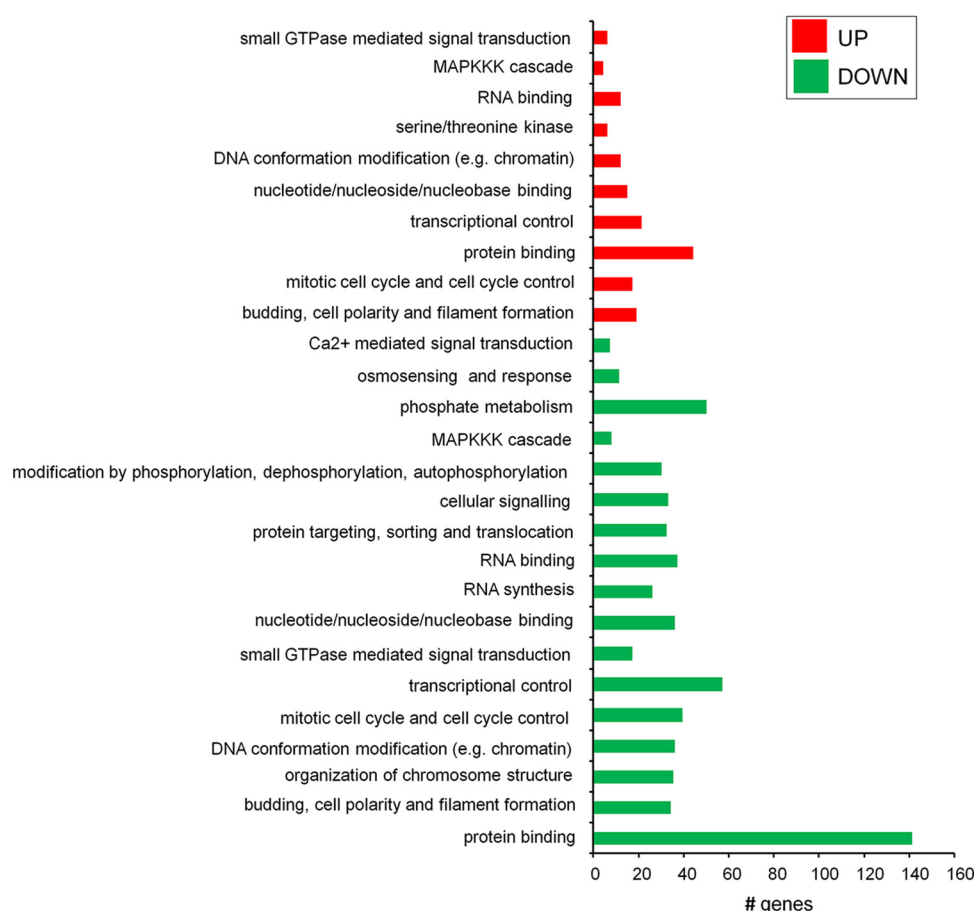


FIG 2 Functional categorization of phosphopeptides differentially phosphorylated in *A. fumigatus* wild-type strain exposed to 2 µg/ml caspofungin treatment for 1 h ($P < 0.05$). The functional enrichment was performed with FungiFun (<https://sbi.hki-jena.de/fungifun/fungifun.php>), using *A. fumigatus* Af293 as the organism and FunCat as the ontology classification.

The results obtained from samples enriched with TiO₂ enrichment for phosphorylated proteins showed a total of 9,613 phosphopeptides, with 6,522 with localization probability levels higher than 75% (class I phosphosites) (Fig. 1A; see also Table S1B). As determined using Student's *t* test, 814 phosphopeptides were differentially expressed between caspofungin-treated wild-type strain and the control (nontreated [0]), with most of them (682 [83.7%]) being dephosphorylated or decreasing their phosphorylation levels (Fig. 1A; see also Table S1B). The analysis of the sites of phosphorylation indicated the presence of 688 residues of serine, 113 residues of threonine, and 13 residues of tyrosine (Fig. 1B) and indicated 1 (641) or 2 (323) phosphosites per peptide (Fig. 1C).

A functional categorization was performed for proteins and phosphopeptides modulated in the wild-type strain during the drug response. Most of the proteins were found to have unknown functions, but four of them were identified as related to the deoxyribonucleotide metabolism (Fig. 1D). A total of 6,030 phosphopeptides modulated in the wild-type response have known function (Fig. 1E). Results of functional categorization of those phosphopeptides are shown in Fig. 2. Functional characterization of proteins that were downregulated and upregulated with respect to phosphorylation in the presence of caspofungin showed high complexity (Fig. 2). Enrichment was seen for proteins that were downregulated and upregulated with respect to phosphorylation and involved in small-GTPase-mediated signal transduction; the MAPK kinase

kinase kinase (MAPKKK) cascade; the mitotic cell cycle; cell cycle control, cell budding, and cell polarity; filament formation; and transcriptional control (Fig. 2). Interestingly, MAPKKK cascade proteins such as BckA^{Bck1}, SskB^{Ssk2}, SteC^{Ste11}, MpkA^{Mpk2}, and SakA^{Hog1} and the MAP phosphatase PtcG (26) were found to be downregulated or upregulated or both (see Table S1 at <https://doi.org/10.6084/m9.figshare.12315212>).

Analysis of the $\Delta mpkA$ and $\Delta sakA$ proteome under the control of the fungal response to caspofungin stress. There is an involvement of MAPKs in the response to caspofungin and the modulation of the CPE (13, 15–17, 27, 28). The study of the global profile of protein levels and of protein phosphorylation in strains deleted for those kinases may provide the identification of new targets related to MAPK signaling pathways and drug responses. Results of a total comparison between proteome and phosphoproteome data from the wild-type (WT caspo/control), $\Delta sakA$ ($\Delta sakA$ caspo/WT caspo), and $\Delta mpkA$ ($\Delta mpkA$ caspo/WT caspo) strains are shown in Fig. 3A (see also Tables S2 and S3 at <https://doi.org/10.6084/m9.figshare.12315212>). The $\Delta mpkA$ strain was found to have the most distinct proteome profile, with a high number of unique proteins modulated, in comparison with WT and $\Delta sakA$ strains (Fig. 3A).

The results of proteomic study of the $\Delta sakA$ mutant strain showed that 11 proteins were not present in $\Delta sakA$ samples (i.e., were exclusively produced by the WT strains under the same treatment conditions), that 72 proteins had decreased intensity in mutant samples, and that 18 proteins had increased total levels (Fig. 3A and B; see also Table S3A at <https://doi.org/10.6084/m9.figshare.12315212>). As shown by $\Delta mpkA$ proteomic data representing results from treatment with caspofungin at 2 μ g/ml, 5 proteins were exclusively produced by the WT samples, and 227 proteins showed a decrease of total level in the mutant strain. Most of the proteins (334) showed increased levels, and 60 proteins were present only in the mutant strain (not found in WT samples) (Fig. 3A and B; see also Table S3A).

In the proteome analysis of the $\Delta mpkA$ mutant strain, the functional enrichment data showed upregulation of proteins involved in electron transport and membrane-associated energy conservation, heat shock proteins, and translational proteins, as previously described (24) (Fig. 3C; see also Table S2B at <https://doi.org/10.6084/m9.figshare.12315212>). For the $\Delta sakA$ proteome, the results showed enrichment in down-regulated proteins involved in glycolysis and gluconeogenesis (7 proteins) and C-compound and carbohydrate metabolism (23 proteins) (see Table S3A).

These data indicate that control of proteins involved in metabolism, such as in production of secondary metabolites, was highly represented in both mutants, suggesting that both kinases were under the control of production of metabolites as a response to caspofungin stress.

Analysis of $\Delta mpkA$ and $\Delta sakA$ phosphoproteome under the control of the fungal response to caspofungin stress. Results of phosphoproteomic analysis of mutants versus wild-type strain indicated a total of 1,217 and 1,235 phosphopeptides showing statistically significant differences in comparisons of the $\Delta mpkA$ mutant to the WT strain ($\Delta mpkA$ /WT) or $\Delta sakA$ /WT, respectively, during 1 h of incubation with 2 μ g/ml caspofungin (Fig. 3A and B; see also Tables S2B and S3B at <https://doi.org/10.6084/m9.figshare.12315212>). A total of 245 phosphoproteins were found to be shared among the wild-type, $\Delta mpkA$, and $\Delta sakA$ strains (Fig. 3B; see also Tables S1, S2B, and S3B). A total of 137 phosphoproteins were unique to the $\Delta mpkA$ mutant, while 88 were unique to the $\Delta sakA$ mutant (Fig. 3B; see also Tables S2B and S3B). There was a predominant decrease in phosphorylation seen for both mutants in comparison with the WT strain. Most (>75%) of the phosphosites identified were serine residues followed by threonine residues and a minimal percentage of tyrosine residues (Fig. 3C). Most of the phosphopeptides were found to have one phosphorylation site per peptide, but four phosphorylation sites per peptide were observed in a few cases (Fig. 3D).

The results of the functional categorization of phosphopeptides from both mutants were very similar and showed a high number of proteins with decreased phosphorylation involved in budding, cell polarity, and filament formation; Ca²⁺-mediated signal transduction; cellular signaling; cytokinesis (cell division)/septum formation and hydrolysis;

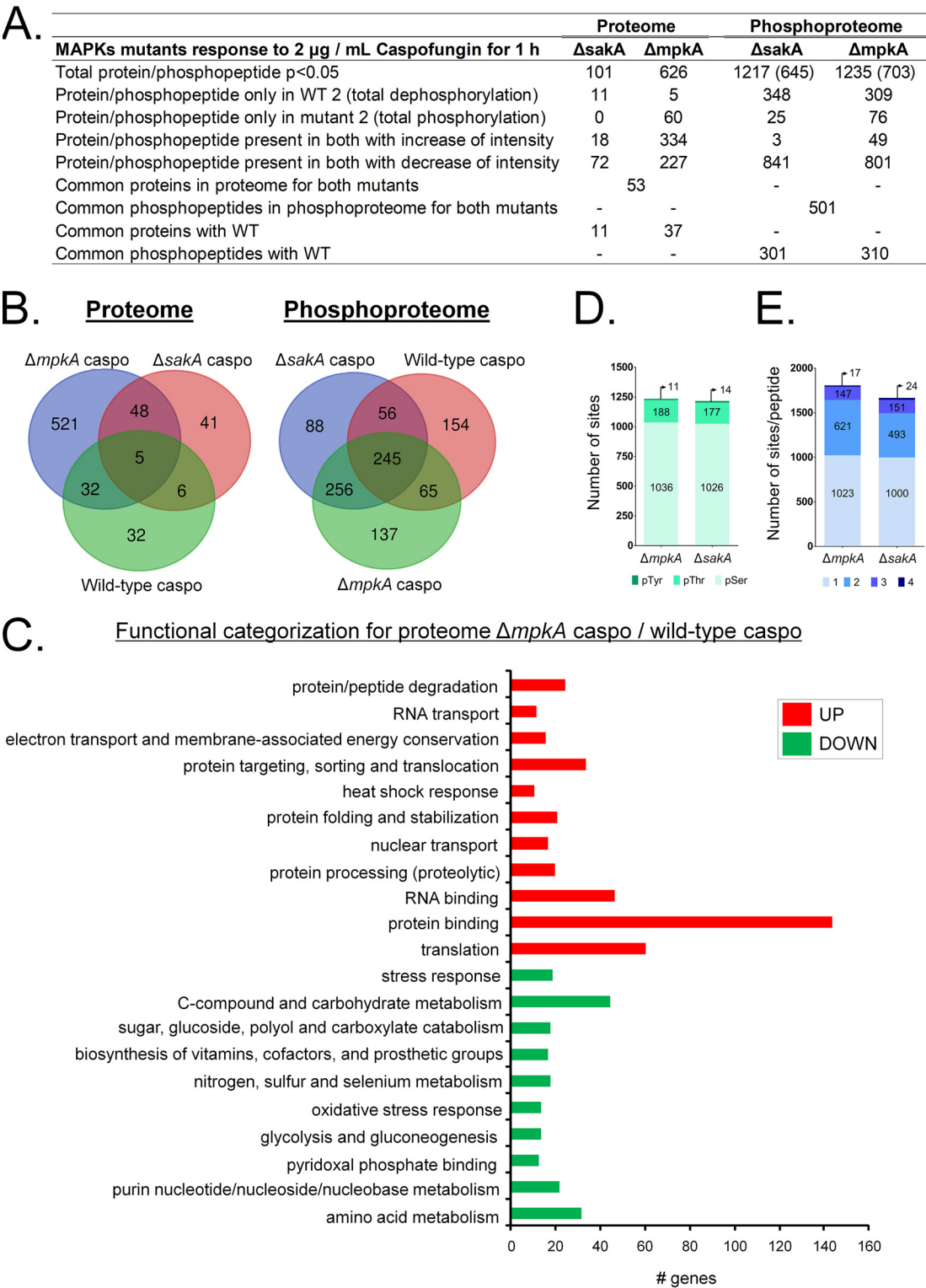


FIG 3 *A. fumigatus* Δ mpkA and Δ sakA proteomic and phosphoproteomic analysis. (A) Summary table of all proteins and phosphopeptides with difference in intensity between mutant samples (Δ mpkA and Δ sakA strains) and the wild-type strain after 2 μ g/ml caspofungin treatment for 1 h ($P < 0.05$). (B) Venn diagram of proteins (proteomes) and phosphopeptides with difference in intensity between mutant (Δ mpkA caspo and Δ sakA caspo) samples and WT samples and between wild-type samples after 2 μ g/ml caspofungin treatment for 1 h and WT samples at time zero (T0) ($P < 0.05$). (C) Functional enrichment was performed with FungiFun (<https://sbi.hki-jena.de/fungifun/fungifun.php>), using *A. fumigatus* Af293 as the organism and FunCat as the ontology classification. (D) Number of phosphorylated residues of serine, threonine, or tyrosine identified after phosphoproteomic analysis for both mutant strains. (E) Number of sites of phosphorylation per peptide for both mutant strains.

the MAPKKK cascade; the mitotic cell cycle; cell cycle control; modification by phosphorylation, dephosphorylation, and autophosphorylation; small-GTPase-mediated signal transduction; and transcriptional control (Fig. 4; see also Table S2B and C). In addition, the $\Delta sakA$ mutant showed decreased phosphorylation of proteins involved in nucleotide/nucleoside/nucleobase binding, regulation of C-compound and carbohydrate metabolism, and RNA synthesis (Fig. 4B; see also Table S2B at <https://doi.org/10.6084/m9.figshare.12315212>).

Taken together, these data strongly suggest that MpkA and SakA collaborate in orchestrating the global phosphorylation of several proteins involved in the response to caspofungin.

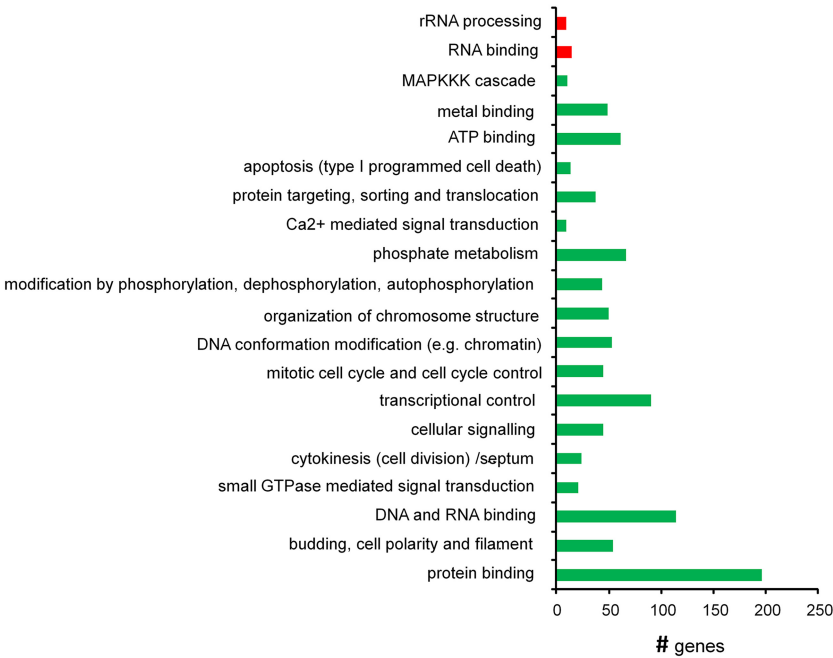
Kinases and transcription factors are involved in the fungal response to caspofungin. Our major interest is in the identification of kinases and transcription factors that may be regulated in *A. fumigatus* during caspofungin responses, which might be under the control of fungal MAPKs. There are 28 kinases modulated in the wild-type strain (Tables 1 and 2). A total of 44 kinases were identified in WT, $\Delta mpkA$, and $\Delta sakA$ samples treated with caspofungin (Table 1). Fourteen kinases were common for all of the strains, 12 kinases were common between the two null mutant strains, and 28 kinases were found to be modulated only during the WT response to caspofungin (Table 1). Table 2 shows the distribution of phosphopeptides in the MAP kinases from the three different MAP kinase modules in the wild-type, $\Delta mpkA$, and $\Delta sakA$ strains upon exposure to caspofungin. All three MAP kinases from the cell wall integrity pathway were found to have phosphopeptides with modulated phosphorylation in the presence of caspofungin (Table 2). MAPKKK SskB and MAPK SakA in the HOG pathway and only the MAPKKK SteC in the invasive growth pathway were also found to have phosphopeptides with modulated phosphorylation (Table 2). Among the kinases exclusively associated with the WT strain, BckA (AFUA_3G11080) is an example of a protein with modulation of two different peptides, one with one site of increased phosphorylation (indicated in bold highlighting) (ESQAPSEGAPDT**SPK**) and a second one with two sites with dephosphorylation (indicated in bold highlighting) (SPRPQDD **SD**ED**S**DDGLFAIPLSN**NK**) (Table 2; see also Table S1B at <https://doi.org/10.6084/m9.figshare.12315212>). The positions of the phosphopeptides indicate that S1039 and S1043 are closer to the active site of the kinase whereas S376 is closer to the N terminus of BckA. The S1039 residue can be phosphorylated by CKII, while the S1043 residue can be a substrate of CKI and CKI I (see Table S1B).

The phosphorylation profiles determined for kinases of the strains after exposure to caspofungin changed dramatically (Tables 1 and 2). In the wild-type strain, most of the kinases showed decreased phosphorylation compared to the untreated control, except for the mitogen-activated protein kinases SskB^{Ssk2} (AFUA_1G10940), SakA^{Hog1} (AFUA_1G12940), and Kic1 (AFUA_2G13640). There was also decreased phosphorylation seen in both the $\Delta mpkA$ mutant (except for AFUA_2G09570 and AFUA_7G03720, Kin28) and the $\Delta sakA$ mutant (Tables 1 and 2). To obtain insight into the integrated kinase signaling networks governing caspofungin phosphoproteomics, we generated functional gene networks using STRING analysis. The protein kinase interaction network generated for the wild-type strain showed not only the MAP kinase subnetwork (SakA^{Hog1}, SskB^{Ssk2}, SteC^{Ste11}, BckA^{Bck1}, and MpkA^{Mpk1}) but also the cAMP-dependent protein kinases Pkar^{Pka1} and SchA^{Sch9} as highly connected (Fig. 5A). Although Pkar^{Pka1} was still present in the $\Delta mpkA$ and $\Delta sakA$ protein kinase interaction network, most of the MAP kinases and SchA^{Sch9}, as well as the corresponding associated proteins, were not present (Fig. 5B and C). These results strongly indicate that MpkA and SakA have an important influence on global phosphorylation during caspofungin tolerance.

There was also a great difference seen in the phosphorylation profiles generated for transcription factors (TFs) among strains postexposure to caspofungin (Table 3). In the wild-type strain, most of the TFs showed decreased phosphorylation compared to the untreated control, except for Sin3 (AFUA_8G05570). There was also decreased phosphorylation in both the $\Delta mpkA$ mutant (except for AFUA_6G09930, Yap1, and AFUA_3G13920, Mbp1) and the $\Delta sakA$ mutant (Table 3). As a first step in characterizing

A.

Phosphoproteome $\Delta mpkA$ caspo / wild-type caspo



B.

Phosphoproteome $\Delta sakA$ caspo / wild-type caspo

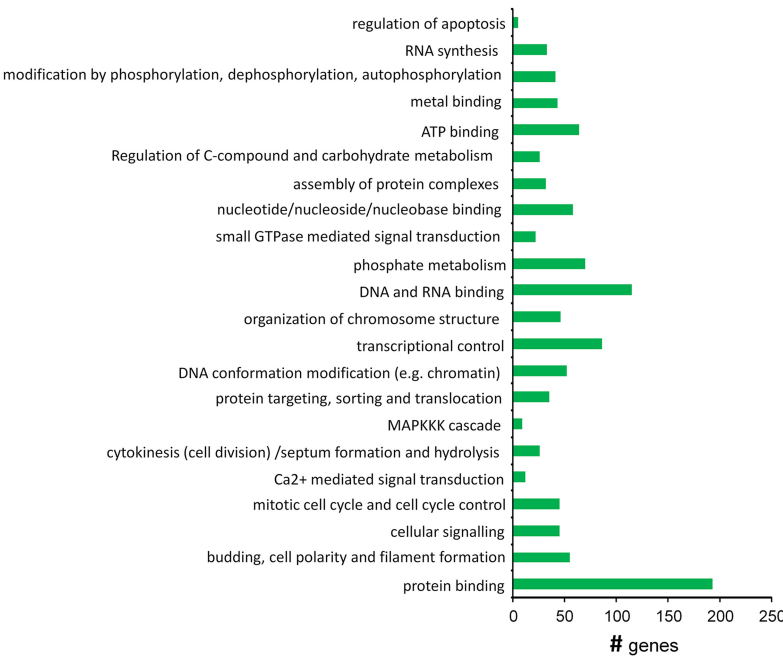


FIG 4 Phosphoproteome functional categorization of *A. fumigatus* $\Delta mpkA$ and $\Delta sakA$ mutants. Functional categorization of phosphopeptides differentially phosphorylated in the $\Delta mpkA$ strain ($P < 0.05$) (A) or $\Delta sakA$ strain ($P < 0.05$) (B) was performed. Functional enrichment was performed with FungiFun (<https://sbi.hki-jena.de/fungifun/fungifun.php>), using *A. fumigatus* Af293 as the organism and FunCat as the ontology classification.

TABLE 1 Protein kinases with modulation of phosphorylation

Gene ID	Gene name	Protein name	Modulation ^a		
			WT caspo/ control	Δ mpkA caspo/ WT	Δ sakA caspo/ WT
AFUA_3G12670	<i>pkh2^b</i>	Serine/threonine protein kinase, putative	↑	↓	↓
AFUA_6G06870	<i>yck2^b</i>	Casein kinase I homolog, putative	↑	↓	↓
AFUA_5G03160	<i>ctk1^b</i>	Protein kinase, putative	↓	↓	↓
AFUA_1G09950	<i>cbkA</i>	Casein kinase II subunit beta (CK II beta)	↓	↓	↓
AFUA_5G11520	<i>nrc2</i>	Serine/threonine protein kinase (Nrc-2), putative (EC 2.7.1.-)	↓	↓	↓
AFUA_5G05980	<i>tos3^b</i>	Calcium/calmodulin dependent protein kinase, putative	↓	↓	↓
AFUA_1G14810	<i>kin4</i>	Serine/threonine protein kinase (Kin4), putative (EC 2.7.11.1)	↓	↓	↓
AFUA_2G12210	<i>sin1</i>	Stress-activated MAP kinase interacting protein, putative	↓	↓	↓
AFUA_3G10000	<i>pkar</i>	cAMP-dependent protein kinase regulatory subunit (PKA regulatory subunit)	↓	↓	↓
AFUA_2G01700	<i>snf1^b</i>	Nonspecific serine/threonine protein kinase (EC 2.7.11.1)	↓	↓	↓
AFUA_5G11840	<i>hrk1^b</i>	Protein kinase, putative (EC 2.7.1.-)	↓	↓	↓
AFUA_2G15010	<i>srrB^c</i>	Serine threonine protein kinase, putative	↓	↓	↓
AFUA_1G11080	<i>kin1</i>	Nonspecific serine/threonine protein kinase (EC 2.7.11.1)	↓	↓	↓
AFUA_6G08120	<i>sldA</i>	Checkpoint protein kinase (SldA), putative	↓	↓	↓
AFUA_2G14200	<i>prk1^b</i>	Protein kinase, putative	—	↓	↓
AFUA_7G04330	<i>ste20^c</i>	Ste20-like serine/threonine protein kinase, putative	—	↓	↓
AFUA_1G11930	<i>nnk1^b</i>	Serine/threonine-protein kinase, putative	—	↓	↓
AFUA_3G08710	<i>isr1^c</i>	Protein kinase domain-containing protein	—	↓	↓
AFUA_4G08920	<i>iks1^b</i>	Protein kinase, putative	—	↓	↓
AFUA_4G06180	<i>ckb1^b</i>	Casein kinase II subunit beta	—	↓	↓
AFUA_5G11970	<i>pkcA</i>	Protein kinase C	—	↓	↓
AFUA_6G04500	<i>gal83^b</i>	Snf1 kinase complex beta-subunit Gal83, putative	—	↓	↓
AFUA_6G09240	<i>ypk2^b</i>	Protein kinase	—	↓	↓
AFUA_1G16780	<i>lkh1</i>	Protein kinase (Lkh1), putative	—	↓	↓
AFUA_1G05800	<i>mkk2</i>	MAP kinase kinase (Mkk2), putative	—	↓	↓
AFUA_6G05120	<i>skp1</i>	Glycogen synthase kinase (Skp1), putative	↓	↓	—
AFUA_4G13720	<i>mpkA</i>	(MpkA) mitogen-activated protein kinase (EC 2.7.11.24)	↓	—	—
AFUA_2G13640	<i>kic1^b</i>	Serine/threonine protein kinase, putative	↑	↓	—
AFUA_1G12940	<i>sakA</i>	(SakA) mitogen-activated protein kinase hog1 (MAP kinase hog1) (EC 2.7.11.24)	↑	—	—
AFUA_2G11730	<i>gin4^b</i>	Protein kinase domain-containing protein	↓	—	—
AFUA_2G16620	<i>gcn2^b</i>	Protein kinase, putative	↓	—	—
AFUA_4G01020	<i>fhk1</i>	Sensor histidine kinase/response regulator, putative (AFU_orthologue AFUA_4G01020)	↓	—	—
AFUA_7G03750	<i>cds1</i>	Serine/threonine-protein kinase chk2 (Cds1)	↑	↓	—
AFUA_1G10940	<i>sskB</i>	MAP kinase kinase kinase (EC 2.7.11.-)	↑	—	—
AFUA_4G03140	<i>sky1</i>	Serine protein kinase Sky1, putative (EC 2.7.1.-)	↑	—	—
AFUA_1G06400	<i>schA</i>	Nonspecific serine/threonine protein kinase (EC 2.7.11.1)	↓	—	—
AFUA_5G06420	<i>steC</i>	MAP kinase kinase kinase SteC (EC 2.7.1.-)	↓	—	—
AFUA_3G11080	<i>bck1</i>	MAP kinase kinase kinase (Bck1), putative	↓	—	—
AFUA_2G01520	<i>yak1^b</i>	Protein kinase, putative	↓	—	—
AFUA_2G09570	<i>stk-55^d</i>	Serine/threonine protein kinase	—	↑	—
AFUA_2G10620	<i>ypk1</i>	Serine/threonine protein kinase (YPK1), putative	—	↓	—
AFUA_7G03720	<i>kin28</i>	Serine/threonine protein kinase (Kin28), putative	—	↑	—
AFUA_1G05930	<i>prk1^b</i>	Serine/threonine protein kinase, putative	—	—	↓
AFUA_2G04680	<i>pakA</i>	Nonspecific serine/threonine protein kinase (EC 2.7.11.1)	—	—	↓

^aThe number of arrows represents the number of phosphopeptides identified for each protein (an arrow pointing down [↓] represents a phosphopeptide that has decreased phosphorylation whereas an arrow pointing up [↑] represents a phosphopeptide that has increased phosphorylation). —, the protein was not found under the described conditions.

^bGene name of orthologs in *S. cerevisiae*.

^cGene name of orthologs in *A. nidulans*.

^dGene name of orthologs in *N. crassa*.

the influence of these TFs on caspofungin tolerance, we analyzed the ability of 13 null mutants of these TFs (29) to grow on caspofungin. We previously observed that a Δ *hapB* mutant (AFUA_2G14720, encoding a CAAT-binding TF) (30) and a Δ *atfA* mutant (AFUA_3G11330) were more susceptible to caspofungin at 0.2 μ g/ml than the wild-type strain and showed reduced CPE (Fig. 6). A Δ *pacC* mutant (AFUA_3G11970, encoding a TF that undergoes activation in response to alkaline pH) (31), and a Δ *zipD* mutant (AFUA_2G03280, encoding a TF important for calcium metabolism and osmotic response) (9, 10), were previously found to have reduced CPE.

TABLE 2 Phosphopeptides observed as differentially modulated in the presence of caspofungin in the mitogen-activated protein kinases^a

Pathway and MAPK	WT caspo/ WT control	$\Delta mpkA$ caspo/ WT caspo	$\Delta sakA$ caspo/ WT caspo	Phosphopeptide
Cell wall integrity MAPKKK BckA (AFUA_3G11080)	Up (2.92)	Down (0.28) Down (0.08) Down	Down (0.26) Down (0.26)	364-ESQAPSEGAPDTS ³⁷⁸ 364-ESQAPSEGAPDTS ³⁷⁸ 364-ESQAPSEGAPDTS ³⁷⁸ 379-LSHEPQSAGPHSGTIENSPNLR-400 798-DAPQHTEGMSPVEGDQQVGISPEPDKADLLAR-829 798-DAPQHTEGMSPVEGDQQVGISPEPDKADLLAR-829 1032-SPRPQDDSD ¹⁰⁵⁶ EDSDGLFAIPLSNK-1056 1032-SPRPQDDSD ¹⁰⁵⁶ EDSDGLFAIPLSNK-1056 1032-SPRPQDDSD ¹⁰⁵⁶ EDSDGLFAIPLSNK-1056
MAPKK Mkk2 (AFUA_1G05800)	Down (0.47)	(Down) 0.31	Down	92-PAPPPLATTGLNESTGH ¹¹⁰ SR-110 92-PAPPPLATTGLNESTGH ¹¹⁰ SR-110
MAPK MpkA (AFUA_4G13720)	Down (0.12) Down (0.16)	(Down) 0.30 Up	Down	173-GFSIDPEENAGYMTEYVATR-192 173-GFSIDPEENAGYMTEYVATR-192 173-GFSIDPEENAGYMTEYVATR-192
Invasive growth MAPKKK SteC (AFUA_5G06420)	Down			584-DSIASSSLQPLQEE ⁶⁰⁵ SPIEPNRK-605
High-osmolarity glycerol MAPKKK SskB (AFUA_1G10940)	Up	Down (0.04)		118-GSSVGAGAALDKVSPVDGLPLTDR-141 118-GSSVGAGAALDKVSPVDGLPLTDR-141
MAPK SakA (AFUA_1G12940)	Up (1.8)			165-IQDPQMTGYVSTR-177

^a"Down" and "Up" represent decreased and increased phosphorylation of a specific phosphopeptide, respectively. Numbers in parentheses represent fold change. MAPK, mitogen-activated protein kinase.

DISCUSSION

Echinocandins, including caspofungin, anidulafungin, and micafungin, represent the second line of treatment for invasive aspergillosis (32, 33). Echinocandins act by the inhibition of the protein Fks1, a component of fungal membrane, resulting in the disruption of the synthesis of the polysaccharide β -(1,3) glucan, a major component of the fungal cell wall (33). In this work, we performed proteome and phosphoproteome analyses of a WT strain and of MAPK null mutants (the $\Delta mpkA$ and $\Delta sakA$ strains) under conditions of high caspofungin concentrations in liquid medium, aiming to identify new targets related to the CPE in *A. fumigatus*. For the analysis of wild-type responses to caspofungin, we identified 814 phosphopeptides (520 unique proteins) with modulation of phosphorylation. Most of the phosphopeptides suffered a decrease of phosphorylation, with a predominance of proteins being related to transcriptional control. The analysis of the response of the $\Delta mpkA$ strain to caspofungin indicates that 1,235 phosphopeptides were being modulated (703 unique proteins), most of them with decreased phosphorylation, such as was observed for the WT response to caspofungin. The modulation of proteins involved in transcriptional control and phosphate metabolism was predominant, as was also observed for the $\Delta sakA$ phosphoproteome.

The participation of MpkA and SakA in the caspofungin response is well established (6, 9, 16, 27). Activation of CWI pathways, together with increased MpkA phosphorylation, occurs at lower concentrations of caspofungin (9). However, under conditions of high concentrations, the phosphorylation of the kinase is reduced (9). In addition, it is known that chitin biosynthesis in *Candida albicans* can be modulated by components of the high-osmolarity glycerol (HOG) pathway (7). It has also been demonstrated that, in *A. fumigatus* treated with subinhibitory concentrations of caspofungin, an *in silico* interaction may occur between SakA and MpkA (16). Here, we showed the involvement of MpkA and SakA in the modulation of phosphorylation of different targets during the response to high doses of caspofungin. We observed that MpkA and SakA suffered dephosphorylation and phosphorylation, respectively, when the wild-type strain was exposed to caspofungin.

Modulation of protein kinases and transcription factors in the response to caspofungin stress was highly represented in all analyses performed. The protein kinase A

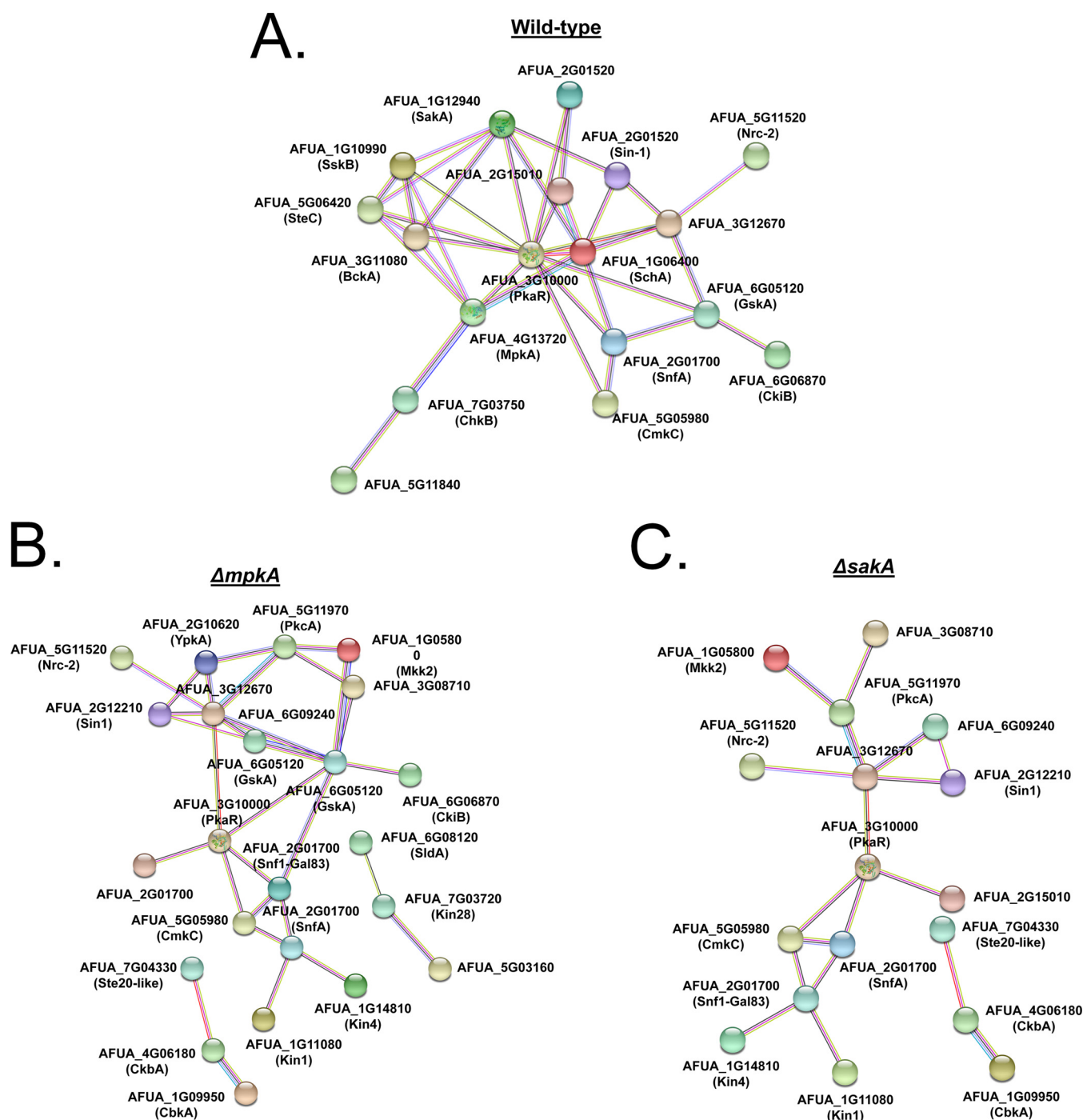


FIG 5 *A. fumigatus* protein kinase functional protein association network based on the protein phosphorylation profile during incubation with caspofungin. The sets of differentially protein kinase phosphorylated proteins from the wild-type (WT) (A), $\Delta mpkA$ (B), and $\Delta sakA$ (C) strains during caspofungin stress were combined for the generation of a general protein association network. Each edge represents a functional protein association retrieved from the STRING server (medium confidence threshold of 0.4 for the interaction score), and node sizes represent the degree of each node (number of edges connected to the node). Note that not all the differentially phosphorylated proteins are present in the network as many proteins did not present any functional associations within the whole set.

(PKA) regulatory subunit (AFUA_3G10000), for example, showed decreased phosphorylation (site indicated in bold highlighting) in the wild-type strain exposed to caspofungin (site **RTSVS**, ratio = 0.5), which was also observed in $\Delta mpkA$ and $\Delta sakA$ phosphoproteomes. In the MAPK null mutant strains, four sites of phosphorylation (indicated with bold highlighting) were identified with dephosphorylation (for the

TABLE 3 Transcription factors with modulation of phosphorylation

Gene ID	Gene name	Protein name	Modulation ^a		
			WT caspo/ control	Δ mpkA caspo/ WT caspo	Δ sakA caspo/ WT caspo
AFUA_3G11970	<i>pacC</i>	C2H2 transcription factor PacC, putative	↓	↓	↓
AFUA_3G11330	<i>atfA</i>	BZIP transcription factor (AtfA), putative	↓	↓	↓
AFUA_1G09670	<i>glcD</i>	HLH transcription factor (GlcD gamma), putative	↓	↓	—
AFUA_3G02340	<i>ncb2^b</i>	CBF/NF-Y family transcription factor, putative	↓	—	↓
AFUA_2G14720	<i>hapB</i>	CCAAT-binding transcription factor subunit HAPB	↓ ↓ ↓	—	↓ ↓ ↓
AFUA_2G03280	<i>zipD</i>	BZIP transcription factor, putative	—	↓ ↓	↓ ↓ ↓
AFUA_2G01900	<i>rtf1p</i>	RNA polymerase II transcription elongation factor Rtf1p, putative	—	↓	↓
AFUA_1G12332	<i>rph1^b</i>	Jumonji family transcription factor, putative	—	↓	↓
AFUA_2G13380	<i>areB</i>	GATA transcription factor (AreB), putative	—	↓	↓ ↓
AFUA_3G11170	<i>csp-2^c</i>	CP2 transcription factor, putative	—	↓ ↓ ↓ ↓	↓
AFUA_2G14250	<i>bur6^b</i>	CBF/NF-Y family transcription factor, putative	—	↓	↓
AFUA_1G12260	<i>iws1</i>	Transcription factor iws1	—	↓	↓
AFUA_5G11390	<i>bqt4^d</i>	APSES transcription factor, putative	—	↓ ↓ ↓ ↓ ↓	↓ ↓ ↓
AFUA_3G08520	<i>rlmA</i>	SRF-type transcription factor RlmA	—	↓	↓
AFUA_5G13310	<i>aro80^b</i>	C6 transcription factor, putative	—	↓	↓
AFUA_8G05570	<i>sin3</i>	Transcription factor (Sin3), putative	↑	—	—
AFUA_1G10760	<i>mak21^b</i>	CCAAT-box-binding transcription factor	↓ ↓	—	—
AFUA_7G04710	<i>fap1^b</i>	NF-X1 finger transcription factor, putative	↓	—	—
AFUA_3G11960	<i>fkh2^b</i>	Forkhead transcription factor Fkh1/2, putative	↓ ↑	—	—
AFUA_1G06900	<i>crzA</i>	C2H2 finger domain transcription factor CrzA	↓	—	—
AFUA_2G17220	<i>amdX</i>	C2H2 transcription factor (AmdX), putative	↓	—	—
AFUA_2G14800	<i>hpa3</i>	HLH transcription factor (HpaIII), putative	↓	—	—
AFUA_5G03430	<i>rum1</i>	PHD transcription factor (Rum1), putative	↓	—	—
AFUA_6G09930	<i>yap1</i>	BZIP transcription factor AP-1/Yap1, putative	—	↑	—
AFUA_3G13920	<i>mbp1^b</i>	APSES transcription factor, putative	—	↓ ↓	—
AFUA_7G05620	<i>mpbA</i>	APSES transcription factor (MbpA), putative	—	↑	—
AFUA_5G04190	<i>palcA</i>	HLH transcription factor (PalcA), putative	—	—	↓

^aThe number of arrows represents the number of phosphopeptides identified for each protein (an arrow pointing down [↓] represents a phosphopeptide that has decreased phosphorylation whereas an arrow pointing up [↑] represents a phosphopeptide that has increased phosphorylation). —, the protein was not found under the described conditions.

^bGene name of ortholog in *S. cerevisiae*.

^cGene name of ortholog in *N. crassa*.

^dGene name of ortholog in *S. pombe*.

Δ sakA phosphoproteome, sites KYSPI [ratio = 0], RTSVS [ratio = 0.12] VTSPT [ratio = 0.13], and PSPS [ratio = 0.28]; for the Δ sakA phosphoproteome, sites PSPS [ratio = 0], KYSPI [ratio = 0], VTSPT [ratio = 0.03], and RTSVS [ratio = 0.06]). There is a physical interaction between *A. fumigatus* SakA and MpkC (17, 34) and the PKA

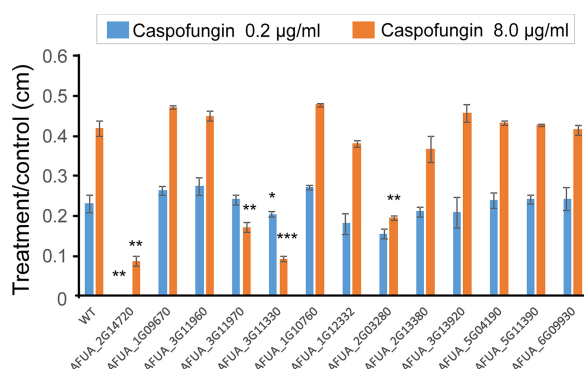


FIG 6 Analysis of *A. fumigatus* null TF strains grown on different concentrations of caspofungin. (A) *A. fumigatus* conidia (1×10^5) were inoculated on solid minimal medium (MM) with different concentrations of caspofungin and grown for 5 days at 37°C. All plates were grown in triplicate, and averages \pm standard deviations (SD) of data were plotted. A Student *t* test was performed using Prism GraphPad (version 6) to confirm the statistical significance of differences between treatment and control results (*, $P < 0.05$; **, $P < 0.01$; ***, $P < 0.001$).

regulatory subunit (35). Carbohydrate mobilization is controlled by SakA interactions with PkaC1 catalytic and PkaR regulatory subunits, suggesting a putative mechanism where the PkaR regulatory subunit leaves the complex and releases the SakA-PkaC1 complex for activation of enzymes involved in carbohydrate mobilization (35). These results suggest a possible participation of PKA, CWI, and HOG pathways in the mobilization of carbohydrate for cell wall remodeling and for responses to caspofungin. In addition, the importance of PKA in fungal viability was also observed in strains deleted for *pkaC1*, which suffered defects in germination and in cell wall organization (36–38). Here, protein kinase C (PKC; AFUA_5G11970) was also identified with dephosphorylation in both the $\Delta mpkA$ and $\Delta sakA$ mutant strains. PKC acts in the CWI pathway in *Saccharomyces cerevisiae* and *A. fumigatus* by the activation of MAPKs with involvement of Bck1 (a MAPKKK, dephosphorylated in WT caspofungin samples), Mkk1/Mkk2 (Mkk2 [AFUA_1G05800], with dephosphorylation in both null mutant strains), and MpkA (AFUA_4G13720, with dephosphorylation only in the WT) (39–43).

Some transcription factors identified here have already been shown to be related to CPE in *A. fumigatus*, such as AtfA (AFUA_3G11330), a homologue of ATF1 (which also includes AtfB or AtfD) (14), with dephosphorylation in the WT, $\Delta mpkA$, and $\Delta sakA$ strains. The ZipD transcription factor (AFUA_2G03280), with dephosphorylation in both mutant strains, also plays a role in the caspofungin-induced CWI response pathway (9, 10). AreB (AFUA_2G13380), with a decrease of phosphorylation in both null mutant strains, was also identified with a modulation of phosphorylation in *A. fumigatus* responses to Congo red (25).

In our study, we demonstrated the complexity of the fungal response to caspofungin stress. The members of the main group of proteins with strong modulation of phosphorylation are related to the transcription control, followed by proteins related to phosphate metabolism and transfer, in which kinases were highly represented. However, the modulation of proteins related to cytoskeletal organization and heat shock responses and β -1,3-glucan synthase is also important; in addition to calcium-calcieneurin pathway and CWI pathways, all of them have already been described in the literature as important for the CPE in *A. fumigatus* and other fungi (7, 8, 10, 19, 28, 44, 45).

Increased understanding of how the modulation of protein phosphorylation may affect the fungal growth in the presence of caspofungin represents an important step in the development of new strategies and methods to combat the fungus inside the host. We showed that the phosphorylation profile is strongly modulated during the drug response, which can be also related to groups of proteins that have already been identified and described as showing level changes during the CPE response (28, 46). We have also shown that the MAPKs MpkA and SakA may control the CPE response by the modulation of the phosphorylation of new targets, which deserves further investigation by future studies.

MATERIALS AND METHODS

Fungal growth, protein extraction, digestion, and phosphoenrichment. *Aspergillus fumigatus* conidia (1×10^7) from the wild-type (WT) strain and mutant strains ($\Delta mpkA$ and $\Delta sakA$ mutants) (strain details are shown in Table S11 at <https://doi.org/10.6084/m9.figshare.12315212>) were inoculated into YG medium {0.5% yeast extract, 1% dextrose, 0.1% trace elements [22.0 g/liter ZnSO_4 , 11 g/liter boric acid, 5 g/liter MnCl_2 , 5 g/liter FeSO_4 , 1.6 g/liter CoCl_2 , 1.6 g/liter CuSO_4 , 1.1 g/liter $(\text{NH}_4)_2\text{MoO}_4$] and incubated for 16 h with rotation at 200 rpm at 37°C. After growth of mycelia, 2 $\mu\text{g}/\text{ml}$ of caspofungin was added to the flasks, followed by incubation for 1 h. Mycelia were filtered using a vacuum system, harvested, and frozen by the use of liquid nitrogen. Frozen mycelia were macerated, resuspended in 1 ml TNE buffer (50 mM Tris-HCl [pH 7.5], 140 mM NaCl, 5 mM EDTA, EDTA-free protease inhibitor cocktail [Roche], 0.1 mM phenylmethylsulfonyl fluoride [PMSF], 100 mM NaF, 1 mM Na_3VO_4 , 0.05 mM sodium β -glycerophosphate) and incubated for 15 min with agitation following centrifugation at $13,000 \times g$ for 10 min. The supernatant was collected and total protein quantified Bradford assay (47). A 500- μg volume of protein was precipitated by addition of trichloroacetic acid (TCA) at a final 10% (wt/vol) concentration, subjected to vortex mixing for 15 s, and placed on ice for a minimum of 30 min. Samples were centrifuged at $14,000 \times g$ for 15 min, and the supernatant was discarded. The pellet was washed three times with cold acetone with centrifugation at $14,000 \times g$ (4°C) for 10 min. Proteins were dissolved in 150 μl of 8 M urea and 50 mM ammonium bicarbonate (Ambic). Dithiothreitol (DTT) (10 mM) was added followed by incubation for 45 min at 30°C. Protein alkylation was performed by addition of 40 mM

iodoacetamide and incubation for 30 min at room temperature in the dark; 5 mM DTT was added with 15 min of incubation at 30°C. Ambic (50 mM) was added for urea dilution, and trypsin was added at a trypsin/protein ratio of 1:50. Protein digestion was performed by an overnight (16-h) incubation at 30°C. The digestion was stopped by addition of trifluoroacetic acid (TFA) to reach a final concentration of 1%. Samples were desalted by the use of an Oasis MCX Plus short cartridge (Waters), and peptide concentrations were determined by the use of a Qubit protein assay kit (Thermo Fisher Scientific). From the total peptides, 5% was collected for proteomic analysis, and 95% was used for phosphopeptide enrichment with TiO₂ resin (Titansphere; GL Sciences Inc., Japan) in batch mode. Samples were resuspended in 80% acetonitrile (ACN)–1 M glycolic acid–5% TFA and mixed into the resin (1 mg resin to 500 µg peptide) and incubated for 20 min at room temperature. Resin was washed three times with 80% ACN–1% TFA, and phosphopeptides were eluted with 0.5% NH₄OH (48, 49).

Nano-LC-MS/MS (nano-liquid chromatography–tandem mass spectrometry) analysis. Peptide samples were resuspended in 0.1% formic acid (FA) before analysis using a nano-flow EASY-nLC 1200 system (Thermo Scientific) coupled to an Orbitrap Fusion Tribrid mass spectrometer (Thermo Scientific) (Instituto de Química, Universidade de São Paulo). The peptides were loaded on an Acclaim PepMap C₁₈ (Thermo Scientific, Germany) trap column (2 cm in length, 100-µm inner diameter; 5-µm pore size) and separated onto an Acclaim PepMap C₁₈ (15 cm in length, 75-µm inner diameter; 3-µm pore size) column and separated with a gradient from 100% mobile phase A (0.1% FA) to 28% phase B (0.1% FA, 80% ACN) for 70 min, 28% to 40% for 10 min, and 40% to 95% for 2 min and 12 min at 95% at a constant flow rate of 300 nL/min. The mass spectrometer was operated in positive-ion mode with data-dependent acquisition. The full scan was acquired in the Orbitrap instrument at a resolution of 120,000 FWHM (full width at half-maximum) in the 375 to 1,600 *m/z* mass range with a maximum injection time of 50 ms and an automatic gain control (AGC) target of 5E–5. Peptide ions were selected using the quadrupole with an isolation window of 1.2 and were fragmented with high-energy collisional dissociation (HCD) MS/MS using a normalized collision energy value of 35 and were detected in the ion trap. Data-dependent acquisition performed with a cycle time of 3 s was used to select the precursor ions for fragmentation. Dynamic exclusion was activated with 12 s as exclusion duration and 20 ppm as the mass tolerance. All raw data were accessed in Xcalibur software (Thermo Scientific).

Database searches and bioinformatics analyses. Raw data were processed using MaxQuant software version 1.5.2.8 and the embedded database search engine Andromeda. The MS/MS spectra were searched against the UniProt *Aspergillus fumigatus* Protein Database (downloaded October 2017; 9,648 entries), with the addition of common contaminants, with accuracies of 4.5 ppm for MS and 0.5 Da for MS/MS. Cysteine carbamidomethylation (57.021 Da) was set as the fixed modification, with two missed cleavages for trypsin. Methionine oxidation (15.994 Da), protein N-terminal acetylation (42.010 Da), and phosphorylation S/T/Y (+79.96 Da) were set as variable modifications. Proteins and peptides were accepted at a false-discovery rate (FDR) of less than 1%. Label-free quantification was performed using MaxQuant software with the “match between run” and iBAQ features activated. The levels of MS intensity of phosphopeptides determined under the different conditions were compared, and the Student *t* test was used for the comparisons. Three biological replicates for each strain were analyzed. Plots of results of principal-coordinate analysis (PCA) comparing all untreated replicates (control) and caspofungin (2 µg/ml)-treated replicates, for proteome or phosphoproteome samples, are indicated in Fig. S1 (available at <https://doi.org/10.6084/m9.figshare.12315212>).

The functional enrichment was performed with FungiFun (<https://sbi.hki-jena.de/fungifun/fungifun.php>), using *A. fumigatus* Af293 as the organism, FunCat as the ontology classification, and identifiers (IDs) from each supplemental table (only “AFUA_” IDs were used). The protein-protein interaction networks were obtained by the use of STRING (<https://string-db.org/>) and Cytoscape version 3.6.1.

ACKNOWLEDGMENTS

This work was funded by grants from Fundação de Amparo à Pesquisa do Estado de São Paulo (FAPESP) to G.H.G. (2016/07870-9), to G.P. (2014/06863-3, 2018/18257-1, 2018/15549-1), and to E.C.M. (2017/19288-5) and by grants from Conselho Nacional de Desenvolvimento Científico e Tecnológico (CNPq) to G.P. and G.H.G.

We thank the two anonymous reviewers for their comments and suggestions.

REFERENCES

- Robbins N, Wright GD, Cowen LE. 2016. Antifungal drugs: the current armamentarium and development of new agents. *Microbiol Spectr* 4(5). <https://doi.org/10.1128/microbiolspec.FUNK-0002-2016>.
- Valiante V, Macheleidt J, Foge M, Brakhage A. 2015. The *Aspergillus fumigatus* cell wall integrity signaling pathway: drug target, compensatory pathways, and virulence. *Front Microbiol* 6:325. <https://doi.org/10.3389/fmicb.2015.00325>.
- Walsh TJ, Anaissie EJ, Denning DW, Herbrecht R, Kontoyiannis DP, Marr KA, Morrison VA, Segal BH, Steinbach WJ, Stevens DA, van Burik JA, Wingard JR, Patterson TF, Infectious Diseases Society of America. 2008. Treatment of aspergillosis: clinical practice guidelines of the Infectious Diseases Society of America. *Clin Infect Dis* 46:327–360. <https://doi.org/10.1086/525258>.
- Arendrup MC, Mavridou E, Mortensen KL, Snelders E, Frimodt-Møller N, Khan H, Melchers WJ, Verweij PE. 2010. Development of azole resistance in *Aspergillus fumigatus* during azole therapy associated with change in virulence. *PLoS One* 5:e10080. <https://doi.org/10.1371/journal.pone.0010080>.
- Stevens DA, White TC, Perlin DS, Selitrennikoff CP. 2005. Studies of the paradoxical effect of caspofungin at high drug concentrations. *Diagn Microbiol Infect Dis* 51:173–178. <https://doi.org/10.1016/j.diagmicrobio.2004.10.006>.
- Steinbach WJ, Lamoth F, Juvvadi PR. 2015. Potential microbiological

- effects of higher dosing of echinocandins. *Clin Infect Dis* 61:S669–S677. <https://doi.org/10.1093/cid/civ725>.
7. Fortwendel JR, Juvvadi PR, Perfect BZ, Rogg LE, Perfect JR, Steinbach WJ. 2010. Transcriptional regulation of chitin synthases by calcineurin controls paradoxical growth of *Aspergillus fumigatus* in response to caspofungin. *Antimicrob Agents Chemother* 54:1555–1563. <https://doi.org/10.1128/AAC.00854-09>.
 8. Juvvadi PR, Muñoz A, Lamoth F, Soderblom EJ, Moseley MA, Read ND, Steinbach WJ. 2015. Calcium-mediated induction of paradoxical growth following caspofungin treatment is associated with calcineurin activation and phosphorylation in *Aspergillus fumigatus*. *Antimicrob Agents Chemother* 59:4946–4955. <https://doi.org/10.1128/AAC.00263-15>.
 9. Ries LNA, Rocha MC, de Castro PA, Silva-Rocha R, Silva RN, Freitas FZ, de Assis LJ, Bertolini MC, Malavazi I, Goldman GH. 2017. The *Aspergillus fumigatus* CrzA transcription factor activates chitin synthase gene expression during the caspofungin paradoxical effect. *mBio* 8:e00705-17. <https://doi.org/10.1128/mBio.00705-17>.
 10. de Castro PA, Colabardini AC, Manfiolli AO, Chiaratto J, Silva LP, Mattos EC, Palmisano G, Almeida F, Persinoti GF, Ries LNA, Mellado L, Rocha MC, Bromley M, Silva RN, de Souza GS, Loures FV, Malavazi I, Brown NA, Goldman GH. 2019. *Aspergillus fumigatus* calcium-responsive transcription factors regulate cell wall architecture promoting stress tolerance, virulence and caspofungin resistance. *PLoS Genet* 15:e1008551. <https://doi.org/10.1371/journal.pgen.1008551>.
 11. Rocha MC, Fabri JH, Franco de Godoy K, Alves de Castro P, Hori JI, Ferreira da Cunha A, Arentshorst M, Ram AF, van den Hondel CA, Goldman GH, Malavazi I. 2016. *Aspergillus fumigatus* MADS-box transcription factor rlmA is required for regulation of the cell wall integrity and virulence. *G3 (Bethesda)* 6:2983–3002. <https://doi.org/10.1534/g3.116.031112>.
 12. Jung US, Sobering AK, Romeo MJ, Levin DE. 2002. Regulation of the yeast Rlm1 transcription factor by the Mpk1 cell wall integrity MAP kinase. *Mol Microbiol* 46:781–789. <https://doi.org/10.1046/j.1365-2958.2002.03198.x>.
 13. Bruder Nascimento AC, Dos Reis TF, de Castro PA, Hori JI, Bom VL, de Assis LJ, Ramalho LN, Rocha MC, Malavazi I, Brown NA, Valiante V, Brakhage AA, Hagiwara D, Goldman GH. 2016. Mitogen activated protein kinases SakA (HOG1) and MpkC collaborate for *Aspergillus fumigatus* virulence. *Mol Microbiol* 100:841–859. <https://doi.org/10.1111/mmi.13354>.
 14. Pereira Silva L, Alves de Castro P, Dos Reis TF, Paziani MH, Von Zeska Kress MR, Riaño-Pachón DM, Hagiwara D, Ries LN, Brown NA, Goldman GH. 2017. Genome-wide transcriptome analysis of *Aspergillus fumigatus* exposed to osmotic stress reveals regulators of osmotic and cell wall stresses that are SakA/HOG1 and MpkC dependent. *Cell Microbiol* 19:e12681. <https://doi.org/10.1111/cmi.12681>.
 15. Manfiolli AO, Siqueira FS, Dos Reis TF, Van Dijk P, Schrevels S, Hoefgen S, Föge M, Straßburger M, de Assis LJ, Heinekamp T, Rocha MC, Janevska S, Brakhage AA, Malavazi I, Goldman GH, Valiante V. 2019. Mitogen-activated protein kinase cross-talk interaction modulates the production of melanins in *Aspergillus fumigatus*. *mBio* 10:e00215-19. <https://doi.org/10.1128/mBio.00215-19>.
 16. Altwasser R, Baldin C, Weber J, Guthke R, Kniemeyer O, Brakhage AA, Linde J, Valiante V. 2015. Network modeling reveals cross talk of MAP kinases during adaptation to caspofungin stress in *Aspergillus fumigatus*. *PLoS One* 10:e0136932. <https://doi.org/10.1371/journal.pone.0136932>.
 17. Manfiolli AO, Mattos EC, de Assis LJ, Silva LP, Ulaş M, Brown NA, Silva-Rocha R, Bayram Ö, Goldman GH. 2019. *Aspergillus fumigatus* high osmolarity glycerol mitogen activated protein kinases SakA and MpkC physically interact during osmotic and cell wall stresses. *Front Microbiol* 10:918. <https://doi.org/10.3389/fmicb.2019.00918>.
 18. Loiko V, Wagener J. 2017. The paradoxical effect of echinocandins in *Aspergillus fumigatus* relies on recovery of the β -1,3-glucan synthase Fks1. *Antimicrob Agents Chemother* 61:e01690-16. <https://doi.org/10.1128/AAC.01690-16>.
 19. Moreno-Velázquez SD, Seidel C, Juvvadi PR, Steinbach WJ, Read ND. 2017. Caspofungin-mediated growth inhibition and paradoxical growth in *Aspergillus fumigatus* involve fungicidal hyphal tip lysis coupled with regenerative intrahyphal growth and dynamic changes in β -1,3-glucan synthase localization. *Antimicrob Agents Chemother* 61:e00710-17. <https://doi.org/10.1128/AAC.00710-17>.
 20. Satish S, Jiménez-Ortigosa C, Zhao Y, Lee MH, Dolgov E, Krüger T, Park S, Denning DW, Kniemeyer O, Brakhage AA, Perlin DS. 2019. Stress-induced changes in the lipid microenvironment of β -(1,3)-d-glucan synthase cause clinically important echinocandin resistance in *Aspergillus fumigatus*. *mBio* 10:e00779-19. <https://doi.org/10.1128/mBio.00779-19>.
 21. Lamoth F, Juvvadi PR, Fortwendel JR, Steinbach WJ. 2012. Heat shock protein 90 is required for conidiation and cell wall integrity in *Aspergillus fumigatus*. *Eukaryot Cell* 11:1324–1332. <https://doi.org/10.1128/EC.00032-12>.
 22. Lamoth F, Juvvadi PR, Soderblom EJ, Moseley MA, Steinbach WJ. 2015. Hsp70 and the cochaperone StiA (Hop) orchestrate Hsp90-mediated caspofungin tolerance in *Aspergillus fumigatus*. *Antimicrob Agents Chemother* 59:4727–4733. <https://doi.org/10.1128/AAC.00946-15>.
 23. Aruanno M, Glampedakis E, Lamoth F. 2019. Echinocandins for the treatment of invasive aspergillosis: from laboratory to bedside. *Antimicrob Agents Chemother* 63:e00399-19. <https://doi.org/10.1128/AAC.00399-19>.
 24. Aruanno M, Bachmann D, Sanglard D, Lamoth F. 2019. Link between heat shock protein 90 and the mitochondrial respiratory chain in the caspofungin stress response of *Aspergillus fumigatus*. *Antimicrob Agents Chemother* 63:e00208-19. <https://doi.org/10.1128/AAC.00208-19>.
 25. Mattos EC, Silva LP, Valero C, de Castro PA, Dos Reis TF, Ribeiro LFC, Marten MR, Silva-Rocha R, Westmann C, da Silva C, Taft CA, Al-Furaiji N, Bromley M, Mortensen UH, Benz JP, Brown NA, Goldman GH. 2020. The *Aspergillus fumigatus* phosphoproteome reveals roles of high-osmolarity glycerol mitogen activated protein kinases in promoting cell wall damage and caspofungin tolerance. *mBio* 11:e02962-19. <https://doi.org/10.1128/mBio.02962-19>.
 26. Winkelströter LK, Bom VL, de Castro PA, Ramalho LN, Goldman MH, Brown NA, Rajendran R, Ramage G, Bovier E, Dos Reis TF, Savoldi M, Hagiwara D, Goldman GH. 2015. High osmolarity glycerol response PtcB phosphatase is important for *Aspergillus fumigatus* virulence. *Mol Microbiol* 96:42–54. <https://doi.org/10.1111/mmi.12919>.
 27. Valiante V, Monteiro MC, Martín J, Altwasser R, El Aouad N, González I, Kniemeyer O, Mellado E, Palomo S, de Pedro N, Pérez-Victoria I, Tormo JR, Vicente F, Reyes F, Genilloud O, Brakhage AA. 2015. Hitting the caspofungin salvage pathway of human-pathogenic fungi with the novel lasso peptide humidimycin (MDN-0010). *Antimicrob Agents Chemother* 59:5145–5153. <https://doi.org/10.1128/AAC.00683-15>.
 28. Conrad T, Kniemeyer O, Henkel SG, Krüger T, Mattern DJ, Valiante V, Guthke R, Jacobsen ID, Brakhage AA, Vlačić S, Linde J. 2018. Module-detection approaches for the integration of multilevel omics data highlight the comprehensive response of *Aspergillus fumigatus* to caspofungin. *BMC Syst Biol* 12:88. <https://doi.org/10.1186/s12918-018-0620-8>.
 29. Furukawa T, van Rhijn N, Fraczek M, Gsaller F, Davies E, Carr P, Gago S, Fortune-Grant R, Rahman S, Gilsenan JM, Houlder E, Kowalski CH, Raj S, Paul S, Cook P, Parker JE, Kelly S, Cramer RA, Latgé JP, Moye-Rowley S, Bignell E, Bowyer P, Bromley MJ. 2020. The negative cofactor 2 complex is a key regulator of drug resistance in *Aspergillus fumigatus*. *Nat Commun* 11:427. <https://doi.org/10.1038/s41467-019-14191-1>.
 30. Blatzer M, Barker BM, Willger SD, Beckmann N, Blosser SJ, Cornish EJ, Mazurie A, Grahl N, Haas H, Cramer RA. 2011. SREBP coordinates iron and ergosterol homeostasis to mediate triazole drug and hypoxia responses in the human fungal pathogen *Aspergillus fumigatus*. *PLoS Genet* 7:e1002374. <https://doi.org/10.1371/journal.pgen.1002374>.
 31. Amich J, Vicentefranqueira R, Leal F, Calera JA. 2010. *Aspergillus fumigatus* survival in alkaline and extreme zinc-limiting environments relies on the induction of a zinc homeostasis system encoded by the *zrfC* and *asp2* genes. *Eukaryot Cell* 9:424–437. <https://doi.org/10.1128/EC.00348-09>.
 32. Denning DW. 2002. Echinocandins: a new class of antifungal. *J Antimicrob Chemother* 49:889–891. <https://doi.org/10.1093/jac/49.4.889>.
 33. Beauvais A, Bruneau JM, Mol PC, Buitrago MJ, Legrand R, Latgé JP. 2001. Glucan synthase complex of *Aspergillus fumigatus*. *J Bacteriol* 183:2273–2279. <https://doi.org/10.1128/JB.183.7.2273-2279.2001>.
 34. Jaimes-Arroyo R, Lara-Rojas F, Bayram Ö, Valerius O, Braus GH, Aguirre J. 2015. The *SrkA* kinase is part of the *SakA* mitogen-activated protein kinase interactome and regulates stress responses and development in *Aspergillus nidulans*. *Eukaryot Cell* 14:495–510. <https://doi.org/10.1128/EC.00277-14>.
 35. de Assis LJ, Manfiolli A, Mattos E, Fabri J, Malavazi I, Jacobsen ID, Brock M, Cramer RA, Thammahong A, Hagiwara D, Ries LNA, Goldman GH. 2018. Protein kinase A and high-osmolarity glycerol response pathways cooperatively control cell wall carbohydrate mobilization in *Aspergillus fumigatus*. *mBio* 9:e01952-18. <https://doi.org/10.1128/mBio.01952-18>.
 36. Grosse C, Heinekamp T, Kniemeyer O, Gehrke A, Brakhage AA. 2008. Protein kinase A regulates growth, sporulation, and pigment formation in *Aspergillus fumigatus*. *Appl Environ Microbiol* 74:4923–4933. <https://doi.org/10.1128/AEM.00470-08>.

37. Fuller KK, Richie DL, Feng X, Krishnan K, Stephens TJ, Wikenheiser-Brokamp KA, Askew DS, Rhodes JC. 2011. Divergent protein kinase A isoforms co-ordinately regulate conidial germination, carbohydrate metabolism and virulence in *Aspergillus fumigatus*. *Mol Microbiol* 79: 1045–1062. <https://doi.org/10.1111/j.1365-2958.2010.07509.x>.
38. Liebmann B, Mu M, Braun A, Brakhage AA. 2004. The cyclic AMP dependent protein kinase A network regulates development and virulence in *Aspergillus fumigatus*. *Infect Immun* 72:5193–5203. <https://doi.org/10.1128/IAI.72.9.5193-5203.2004>.
39. Rocha MC, Godoy KF, de Castro PA, Hori JI, Bom VL, Brown NA, Cunha AF, Goldman GH, Malavazi I. 2015. The *Aspergillus fumigatus* pkcAG579R mutant is defective in the activation of the cell wall integrity pathway but is dispensable for virulence in a neutropenic mouse infection model. *PLoS One* 10:e0135195. <https://doi.org/10.1371/journal.pone.0135195>.
40. Dichtl K, Helmschrott C, Dirr F, Wagener J. 2012. Deciphering cell wall integrity signalling in *Aspergillus fumigatus*: identification and functional characterization of cell wall stress sensors and relevant Rho GTPases. *Mol Microbiol* 83:506–519. <https://doi.org/10.1111/j.1365-2958.2011.07946.x>.
41. Irie K, Takase M, Lee KS, Levin DE, Araki H, Matsumoto K, Oshima Y. 1993. MKK1 and MKK2, which encode *Saccharomyces cerevisiae* mitogen-activated protein kinase-kinase homologs, function in the pathway mediated by protein kinase C. *Mol Cell Biol* 13:3076–3083. <https://doi.org/10.1128/mcb.13.5.3076>.
42. Lee KS, Levin DE. 1992. Dominant mutations in a gene encoding a putative protein kinase (BCK1) bypass the requirement for a *Saccharomyces cerevisiae* protein kinase C homolog. *Mol Cell Biol* 12:172–182. <https://doi.org/10.1128/mcb.12.1.172>.
43. Gustin MC, Albertyn J, Alexander M, Davenport K. 1998. MAP kinase pathways in the yeast *Saccharomyces cerevisiae*. *Microbiol Mol Biol Rev* 62:1264–1300. <https://doi.org/10.1128/MMBR.62.4.1264-1300.1998>.
44. Kaneko Y, Ohno H, Imamura Y, Kohno S, Miyazaki Y. 2009. The effects of an Hsp90 inhibitor on the paradoxical effect. *Jpn J Infect Dis* 62:392–393.
45. Wiederhold NP, Kontoyiannis DP, Prince RA, Lewis RE. 2005. Attenuation of the activity of caspofungin at high concentrations against *Candida albicans*: possible role of cell wall integrity and calcineurin pathways. *Antimicrob Agents Chemother* 49:5146–5148. <https://doi.org/10.1128/AAC.49.12.5146-5148.2005>.
46. Cagas SE, Jain MR, Li H, Perlin DS. 2011. Profiling the *Aspergillus fumigatus* proteome in response to caspofungin. *Antimicrob Agents Chemother* 55:146–154. <https://doi.org/10.1128/AAC.00884-10>.
47. Bradford MM. 1976. A rapid and sensitive method for the quantitation of microgram quantities of protein utilizing the principle of protein-dye binding. *Anal Biochem* 72:248–254. <https://doi.org/10.1006/abio.1976.9999>.
48. Larsen MR, Thingholm TE, Jensen ON, Roepstorff P, Jørgensen TJ. 2005. Highly selective enrichment of phosphorylated peptides from peptide mixtures using titanium dioxide microcolumns. *Mol Cell Proteomics* 4:873–886. <https://doi.org/10.1074/mcp.T500007-MCP200>.
49. Palmisano G, Parker BL, Engholm-Keller K, Lendal SE, Kulej K, Schulz M, Schwämmle V, Graham ME, Saxtorph H, Cordwell SJ, Larsen MR. 2012. A novel method for the simultaneous enrichment, identification, and quantification of phosphopeptides and sialylated glycopeptides applied to a temporal profile of mouse brain development. *Mol Cell Proteomics* 11:1191–1202. <https://doi.org/10.1074/mcp.M112.017509>.